B1 − 8

Quantitative Reconstruction for ^{99m}Tc Source Distribution in Uniform Attenuating Medium

Hiroyuki Shinohara, Tomoaki Yamamoto, Yoshio Kuniyasu, Takeyuki Hashimoto[1], Munehiro Takahashi[2] and Takashi Yokoi[2]

Dept. of Radiology, Showa University Fujigaoka Hospital, [1] Dept. of Image Processing, Yokohama Soei College, [2] Dept. of Medical Systems, Shimadzu Corporation

1. INTRODUCTION

Exact methods of inverting the two-dimensional (2-D) exponential Radon transform were proposed by Bellini et al (1979) and Inouye et al (1989), both of whom worked in the spatial frequency domain to estimate the 2-D Fourier transform (2D-FT) of an unattenuated sinogram; by Hawkins et al (1988), who worked with circular cylinders harmonic Bessel transforms; and by Tretiak and Metz (1980), who performed exponentially-weighted backprojection after filtering of appropriately-modified projections. Metz and Pan (1995)[1] and Kudo and Saito (1996)[2] developed a generalized theory that all these methods can be interpreted as special cases of a broad class of the 2-D FT of a modified sinogram. Moreover, they proposed a new "quasi-optimal" method that is predicted to have noise properties better than those of previously-proposed methods. Theoretical and numerical simulation studies demonstrated that the quasi-optimal method achieves smaller global variance in the reconstructed images than do the other methods of the class. However, the quantitative accuracy of exact methods in determining realistic activity concentration in a uniform attenuating medium has not been reported.

In the present study, we investigated the accuracy of activity concentration and image contrast reconstructed with the Bellini, Inouye, and quasi-optimal methods (Metz-Pan method) for extended source distribution.

2. METHOD

2-1. Analytical attenuation correction methods

For a uniform attenuating medium, the attenuated sinogram that arise in conventional 2-D SPECT with parallel projections of a distribution of radioactivity, a(x,y), is given by

$$p(\xi,\phi;\mu) = \int_{\eta=-\infty}^{\infty} a(\xi\cos\phi - \eta\sin\phi, \xi\sin\phi + \eta\cos\phi) \cdot e^{-\mu[\eta + D(\xi,\phi)]}\, d\eta, \tag{1}$$

where μ (real and > 0) denotes the linear attenuation coefficient inside the attenuator, $\xi = x\cos\phi + y\sin\phi$ and $\eta = -x\sin\phi + y\cos\phi$ represent Cartesian coordinates in a system that is rotated through angle ϕ relative to the (x,y) system and $D(\xi,\phi)$ represents the distance from the point ($x = \xi\cos\phi$, $y = \xi\sin\phi$) to the boundary of the attenuator in the projection, as shown in figure 1. The modified attenuated sinogram can be defined as

$$m(\xi,\phi;\mu) = e^{\mu D(\xi,\phi)} \cdot p(\xi,\phi;\mu). \tag{2}$$

The 2-D FT of the unattenuated sinogram $p(\xi,\phi)$ ($\mu = 0$ equation (1)) is defined as

$$A_k(\nu_a) \equiv \frac{1}{2\pi} \int_{\phi=0}^{2\pi} \int_{\xi=-\infty}^{\infty} p(\xi,\phi)\, e^{-jk\phi}\, e^{-j2\pi\nu_a\xi}\, d\xi\, d\phi, \tag{3}$$

where ν_a is the spatial frequency variable and k is the spatial index.

The unified analytical attenuation correction formula for a uniform attenuator of Metz and Pan is given by

$$A_k^n(\nu_a) = \frac{\gamma^{-(n-1)k}}{\gamma^{-nk} + \gamma^{nk}} M_k(\nu_m) + (-1)^k \frac{\gamma^{(n-1)k}}{\gamma^{-nk} + \gamma^{nk}} M_k(-\nu_m), \tag{4}$$

where $M_k(\nu_m)$ is the 2-D FT of the modified attenuated sinogram, $\nu_m = \sqrt{\nu_a^2 + \nu_\mu^2}$ ($\nu_\mu = \mu/2\pi$) and γ is the spatial frequency variable defined as

$$\gamma \equiv \frac{\sqrt{\nu_m^2 - \nu_\mu^2}}{\nu_m + \nu_\mu}. \tag{5}$$

By setting n = 1, equation (4) reduces to the Bellini formula; setting $n \rightarrow \infty$ reduces the equation to the Inouye formula; and setting n = 2 reduces the equation to the Metz-Pan formula. Equation (4) is valid only for $k \geq 0$ and $\nu_a \geq 0$, and that the values of $A_k(\nu_a)$ in the other three quadrants of the (ν_a, k) plane are given by equation (24) in Metz and Pan (1995).

2-2. Phantom and data acquisition

The phantom shown in figure 2(b) had the shape of a pie-chart divided into six cavities, each 480 ml in volume and 10 cm in height, that were symmetrically positioned in a cylinder that was 20 cm in diameter and 10 cm in height. This phantom tests for linearity between true activity concentration and measured activity concentration, and it is denoted as linearity phantom in the present study. Each cavity contained a different concentration of homogeneous solution of ^{99m}Tc (74, 148, 222, 296, 370, and 444 kBq ml^{-1}).

Figure 1

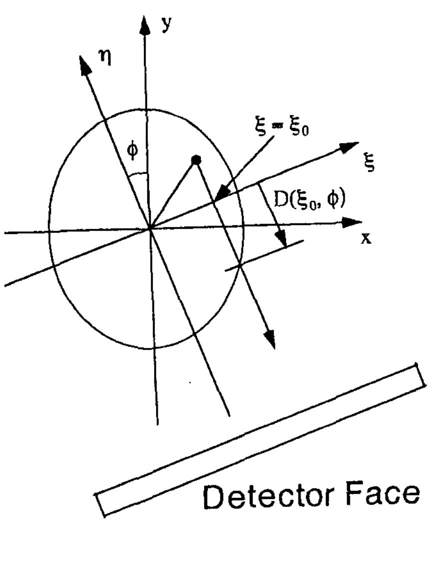

Figure 2

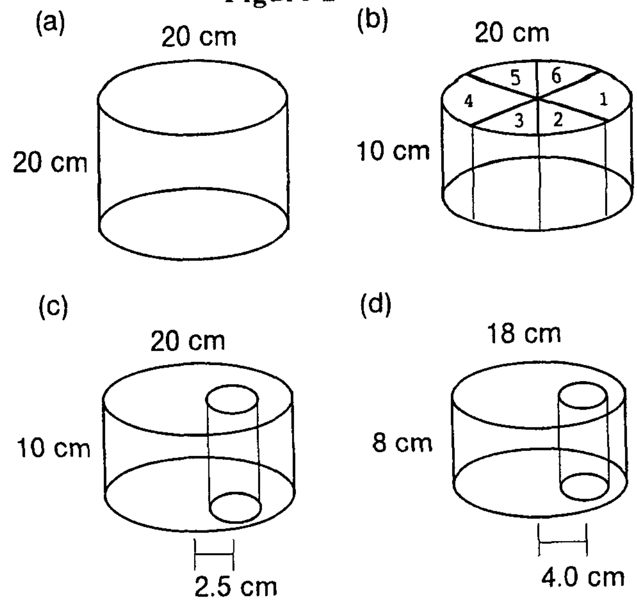

The phantom shown in figure 2(c) contains a "water cylinder" insert (diameter, 5.5 cm and height, 10 cm) positioned 2.5 cm from the centre of the 20 × 10 cm cylinder that is filled with homogeneous solution of ^{99m}Tc (318 kBq ml^{-1}). This phantom was used to evaluate the image contrast of cold region and was denoted as cold-rod phantom 1 in the present study. The phantom shown in figure 2(d) contains a different "water cylinder" insert (diameter, 5.5 cm and height, 8 cm) positioned 4.0 cm from the centre of a different cylinder (18 cm in diameter and 8 cm in height) that is filled with homogeneous solution of ^{99m}Tc (318 kBq ml^{-1}). This second phantom was also used to evaluate the image contrast of cold region and was denoted as cold-rod phantom 2.

A three-headed, rotating SPECT gamma camera (PRISM 3000, Picker International, Bedford, OH) with a low-energy ultra-high-resolution parallel (LEUHR) collimator was used. Projections were acquired in a 128 × 128 matrix (pixel length 3.56 mm), in 3° steps over the 360° circular orbit with a radius of 19 cm for 10 sec per step; total scan time was 20 min. Each of three detectors collected 40 views during 120 degrees of rotation. Data acquisition was performed with two energy windows: a 20% photopeak energy window set symmetrically over the 140-keV peak of ^{99m}Tc and a secondary 5% energy window set over 122-keV peak.

2-3. Scatter correction

Energy subtraction scatter correction method is expressed as

$$p(\xi,\phi;\mu) = p_1(\xi,\phi;\mu) - k\ p_2(\xi,\phi;\mu), \qquad (6)$$

where k is a constant determined in the setting of photopeak (p_1) and secondary energy windows (p_2). The k value for accurate scatter correction may vary depending on the energy resolution of the gamma camera and geometric design of collimator as well as object size and source distribution. We optimized k for the PRISM 3000-LEUHR collimator system with phantom experiments to perform quantitative evaluation of the three analytical attenuation correction methods.

First we set k = 0 in equation (6) and reconstructed the linearity phantom image with the Metz-Pan method. Before processing, the projections of photopeak energy window were smoothed with a Butterworth filter of order 4 and a cut-off frequency of 0.4 cycles pixel^{-1}. The projections of secondary energy window were smoothed with the Butterworth filter of order 4 and a cut-off frequency of 0.18 cycles pixel^{-1}. The relation between ^{99m}Tc activity concentration (x) and the count density of each cavity region (y) was fitted to a line using the least squares method so that

$$y = ax + b. \qquad (7)$$

If scatter correction is not done, the y-intercept (b) corresponding to no activity is not zero. If scatter correction is perfect, b should be zero. Since the analytical attenuation correction method is a linear operation, b is proportional to k, so that we can easily find k for which b is nearly equal to zero. We determined that k = 2.1 was the optimized k for the PRISM 3000-LEUHR collimator system.

The validity of the k, if it was applied to another phantom-containing cold region, was investigated using cold-rod phantom 1 and cold-rod phantom 2 that had different object sizes and positions in the cold region.

3. RESULTS

Figure 3 shows the relation between activity concentration (x) and count density of a linearity phantom image (y) reconstructed with the Metz-Pan method with and without scatter-corrected projections. Validity of the k was evident from the fact that y-intercept of 40.6 counts pixel-1 without scatter correction (y = 40.6 + 3.05x; R^2 = 0.999) decreased to 0.23 counts pixel-1 (y = 0.23 + 2.44x; R^2 = 0.999) with scatter correction. If we did not optimize the k and the TEW method was used, the regression line was given as y = -7.52 + 2.4048x (R^2 = 0.999), showing excessive subtraction.

Figure 4 shows the relation between true activity concentration (x) and measured activity concentration (y). If scatter correction was not performed, the y-intercept had 11.4 kBq ml-1, and the slope was smaller than 1 (y = 11.4 + 0.897x; R^2 = 0.999). With scatter correction, the y-intercept decreased to only 0.1 kBq ml-1, and the slope was nearly equal to 1 (y = 0.09 + 1.0241x; R^2 = 0.999). Regression lines were y = 0.63 + 1.0255x (R^2= 0.9987), y = -2.62 + 1.0278x (R^2 = 0.9995), and y = 0.092 + 1.0241x (R^2= 0.9989) for the Bellini, Inouye, and Metz-Pan methods respectively[3]. Contrast of a cold region in the cold-rod phantom 1 and 2 was 96% and 101% for all three methods.

Figure 3

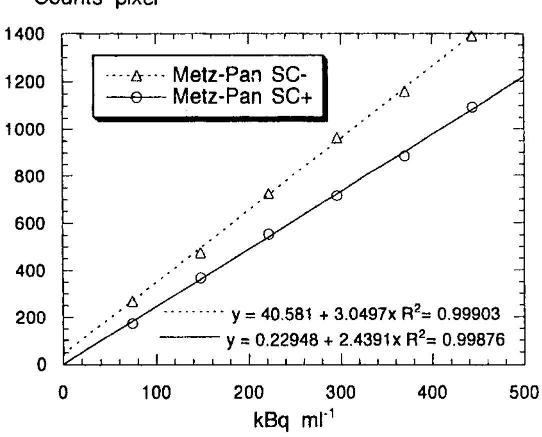

Figure 4

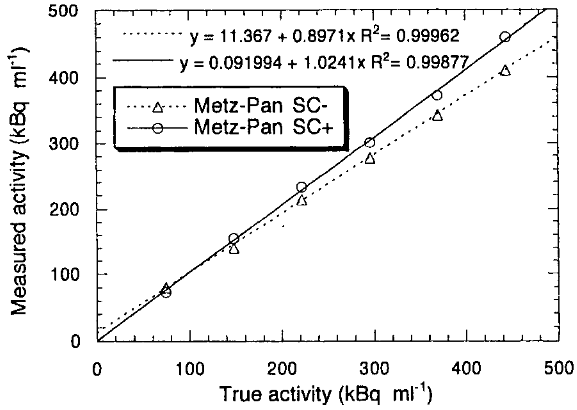

4. DISCUSSION

We performed the same linearity phantom experiment for a PRISM 3000 with low-energy ultra-high resolution fan beam (LEUHRF) collimator and obtained another a k value that differed from k = 2.1, the value for the PRISM 3000-LEUHR collimator system. These results indicate that the scatter effect varied depending upon the combination of gamma camera and collimator used, and thus optimization of k is required to perform accurate scatter correction.

5. CONCLUSION

Combined optimized scatter correction and analytical attenuation correction methods achieve good accuracy in quantification of activity distribution with a uniform attenuating medium.

References

1) Metz C E and Pan X: A unified analysis of exact methods of inverting the 2-D exponential Radon transform, with implications for noise control in SPECT IEEE Trans. Med. Imaging **MI-14:** 643-58, 1995
2) Kudo H and Saito T: Unification and noise propagation property of analytical SPECT reconstruction methods IEICETrans. Inf. and Syst. **J79-D-II:** 977-88, 1996
3) Shinohara H, Matsuoka S, 'Yamamoto T, et al.: Implementation and quantitative evaluation of analytical methods for attenuation correction in SPECT: Phantom study. J. Nucl. Med. **40:** 304, 1999 (Abstract).